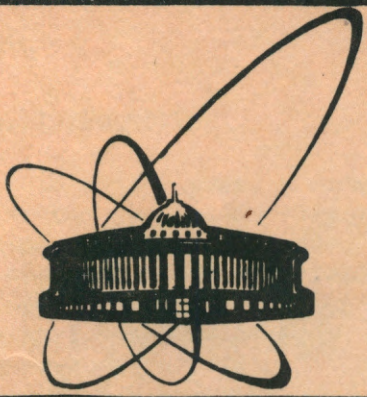

сообщения
объединенного
института
ядерных
исследований
дубна



E1-89-252

P.Kozma, C.Damdinsuren, D.Chultem*,
B.Tumendemberel*

# NUCLEAR REACTIONS OF TANTALUM WITH 3.65 AGeV $^{12}$C-IONS AND 3.65 GeV PROTONS

Submitted to "Nuclear Physics A"

* Mongolian State University, Ulan-Bator, Mongolia

1989

## 1. INTRODUCTION

In recent years a considerable experimental effort has been devoted to the investigation of nuclear reactions induced by high-energy projectiles[1]. Such investigations yield valuable information for understanding the reaction mechanism and nuclear properties, but can also be useful for testing the fundamental concepts of high-energy physics.The interaction of high-energy projectiles with complex nuclei can be understood in terms of a two-step mechanism in which the excitation and de-excitation stages are assumed. Experimental data are obviously discussed in the framework of two extreme concepts of the reaction mechanism: the abrasion-ablation[2] and the intranuclear cascade[3,4] models. These model representations can be used to calculate the mass distributions of target residues in these interactions.

Two basic hypotheses of high-energy physics[5,6] can also be discussed. The hypothesis of factorization (scaling) predicts that both the spectra and yields of a given fragment can be described as a product of a target or projectile factor. The distribution of fragments is independent of the projectile except for a constant term projectile factor. The second one, limiting fragmentation, predicts that the energy spectra and cross sections of residues in their proper frame (either a projectile or a target) are independent of bombarding energy at sufficiently high energies.

In this context a careful and systematic experimental study of the distribution of residues produced in nuclear reactions induced by high-energy projectile is desirable. Particularly, it is worthwile to investigate the yields of products formed in relativistic heavy-ion interactions with those produced in proton-induced reactions at the same AGeV energy. Using this motivation, we have undertaken a study of the nuclear reactions induced by 3.65 AGeV $^{12}C$-ions and 3.65 GeV protons with tantalum target nuclei using the foil stack action technique and Ge(Li) gamma-ray spectroscopy. This experimental technique is unique as regards the identification of a variety of residues, the products of spallation and target fragmentation. A large number of heavy target residues forms a good statistical basis

for obtaining their charge and mass distributions, as well. In view of both basic concepts and reaction mechanisms these results and their analysis are important. Moreover, the availability at the Dubna synchrophasotron to accelerate the $^{12}C$-ions and protons with the same A GeV energy allows one to make a comparison with earlier studies of the tantalum target fragmentation by intermediate 0.34-0.66 GeV [7-9], 5.7 GeV [10] and 8.1 GeV [11] proton energies, respectively, as well as to gain new experimental results: to date the nuclear reactions of tantalum with high-energy $^{12}C$-ions have not been experimentally studied.

The paper is organized as follows. The experimental procedure is described in Sect.2. The results are presented in Sect. 3, i.e. nuclidic cross sections and their parametrization which gives charge dispersions and isobaric yields of target residues in both experiments. Here, the measured recoil properties of intermediate fragments as well as effects of secondary particle induced reactions are also given. Sect. 4 deals with the test of fundamental hypotheses (factorization, limiting fragmentation) regarding to present and previous results. In Sect. 5 we compare mass-yield distributions with the abrasion-ablation and intranuclear cascade model calculations. Finally, Sect. 6 contains our conclusions.

## 2. EXPERIMENTAL

Target stacks containing Mylar, aluminium and tantalum foils of high purity (99.99%) were irradiated with 3.65 AGeV $^{12}C$-ions and 3.65 GeV protons in an external beam of the Dubna synchrophasotron. The target discs were 5 cm in diameter and their thicknesses were as indicated in table 1. The target stacks, positioned so that the beam passed through the centre, were exposed to $^{12}C$-ion and proton beams with a total intensity of about $10^{13}$. Aluminium foils No.2 in both target stacks were used as beam flux monitors by measuring the induced $^{24}Na$ activity. The cross sections of the monitor reactions $^{27}Al(p,X)^{24}Na$ and $^{27}Al(^{12}C,X)^{24}Na$ were taken to be $8.7 \pm 0.8$ mb and $19.0 \pm 1.5$ mb [12], respectively.

The targets were gamma-ray counted on the Ge(Li) spectrometer with 4096 channel capacity. The resolution of three Ge(Li) detectors used (28 $cm^3$, 45 $cm^3$ and 50 $cm^3$) was 2.8 keV, 2.3 keV, and 2.5 keV, respectively. They were calibrated for absolute efficiencies with a variety of gamma-ray standards: based on



Table 1. Properties of the target stacks

| Foil | Material | Thickness ($mg/cm^2$) for proton beam | $^{12}C$-ion beam |
|---|---|---|---|
| 1 | Al | 19.5 | 20.1 |
| 2 | Al | 20.0 | 20.0 |
| 3 | Al | 20.0 | 19.8 |
| 4 | My | 17.6 | 17.5 |
| 5 | Ta | 62.1 | 61.9 |
| 6 | Ta | 154.2 | 154.0 |
| 7 | Ta | 61.8 | 62.0 |
| 8 | My | 17.5 | 17.5 |

the deviations of individual calibration points from a smooth curve the absolute accuracy of the calculations was estimated to be about 5%. The spectra were analyzed with a computer code SAMPO [13]. The radionuclides were unambiguously identified by their gamma-ray energies, half-lives and fractional abundances [14].

## 3. RESULTS

### 3.1. Secondary effects

The contribution of secondary particle induced reactions to the nuclidic cross sections was estimated from the ratio of the production cross sections measured simultaneously with the thick and thin tantalum targets. Fig. 1 shows the ratio obtained for these two targets in both experiments as a function of product mass number. The ratios for both reactions were found to be independent of mass number for products with $A \lesssim 150$; the average value of the thick to thin target cross section ratios fluctuates about unity. It indi-

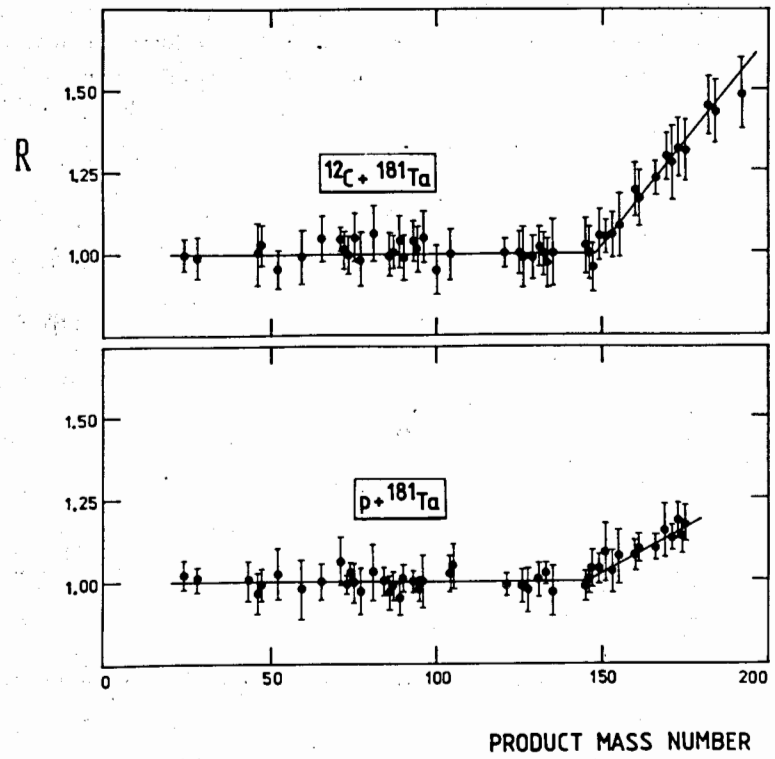


Fig. 1. Thick to thin target cross section ratios $R = \sigma(154\ mg/cm^2)/\sigma(62\ mg/cm^2)$ from the $^{12}C + ^{181}Ta$ and reactions at 3.65 AGeV, respectively.

cates that secondary effects for these products are negligible. On the other hand, the experimental ratios for products $A \geq 150$ sharply increase with product mass number. It shows the occurrence of visible secondary effects for nuclides produced close to the target number. The nuclidic cross sections in this mass region were corrected for the contribution of secondaries by linear extrapolation to zero target thickness.

### 3.2. Nuclidic Cross Sections

The nuclidic cross sections are listed in table 2. The errors assigned to the cross section values are based on those of counting statistics, detector efficiences and target thicknesses, as well. The systematic error of about 10% corresponding to the beam flux monitor is not included.



Table 2. Cross sections for the production of target residues in the reactions of tantalum with 3.65 AGeV $^{12}C$-ions and protons. Symbols I and C are used for independent and cumulative yields, respectively.

| Nuclide | Type of yield | Protons (mb) | $^{12}C$-ions (mb) |
|---|---|---|---|
| 1 | 2 | 3 | 4 |
| $^{24}Na$ | C | 7.5±0.5 | 36.4±3.3 |
| $^{28}Mg$ | C | 2.9±0.2 | 12.1±0.9 |
| $^{43}K$ | C | 1.5±0.2 | |
| $^{46}Sc$ | I | 6.3±1.0 | 13.7±2.9 |
| $^{48}Sc$ | I | 0.8±0.2 | 3.4±0.7 |
| $^{52}Mn$ | C | 0.7±0.1 | 1.8±0.4 |
| $^{59}Fe$ | C | 1.0±0.2 | 2.7±0.7 |
| $^{65}Zn$ | C | 3.9±0.6 | 10.5±1.4 |
| $^{72}Ga$ | C | | 6.8±1.2 |
| $^{73}Ga$ | C | | 4.0±1.1 |
| $^{71}As$ | C | 2.7±0.2 | 6.8±0.7 |
| $^{74}As$ | I | 2.5±0.2 | 7.3±0.9 |
| $^{73}Se$ | C | 1.0±0.2 | |
| $^{75}Se$ | C | 2.9±0.8 | 7.7±1.8 |
| $^{77}Br$ | C | 4.2±1.0 | |
| $^{81}Rb$ | C | 3.6±0.3 | 7.9±0.8 |
| $^{82}Rb^m$ | C | 1.7±0.4 | 6.0±1.5 |
| $^{84}Rb$ | I | 0.6±0.1 | 2.1±0.5 |
| $^{84}Rb^m$ | I | 0.8±0.2 | |

Table 2 (continued)

| 1 | 2 | 3 | 4 |
|---|---|---|---|
| $^{86}Y$ | C | 3.9±0.6 | 8.2±1.4 |
| $^{87}Y$ | C | 2.8±0.2 | |
| $^{87}Y^{m}$ | C | 3.4±0.5 | 11.6±1.9 |
| $^{86}Zr$ | C | 1.5±0.2 | 1.9±0.4 |
| $^{89}Nb$ | C | 2.3±0.2 | 5.2±0.7 |
| $^{90}Nb$ | C | 2.1±0.3 | 6.4±1.1 |
| $^{93}Tc$ | C | 1.3±0.2 | 2.1±0.4 |
| $^{94}Tc$ | I | 1.4±0.2 | 2.6±0.6 |
| $^{95}Tc$ | C | 3.7±0.3 | |
| $^{101}Rh^{m}$ | C | 2.9±0.3 | |
| $^{100}Rh$ | I | | 13.0±2.6 |
| $^{104}Ag$ | C | 2.5±0.6 | 5.0±1.4 |
| $^{105}Ag$ | C | 4.8±0.6 | |
| $^{125}Sn$ | C | | 7.1±2.2 |
| $^{118}Sb^{m}$ | C | | 3.6±1.2 |
| $^{126}Sb$ | C | 3.9±0.9 | 6.9±1.8 |
| $^{127}Sb$ | C | 7.0±1.3 | 11.2±2.1 |
| $^{121}Te$ | C | 6.1±0.7 | |
| $^{129}Cs$ | C | 7.6±0.9 | |
| $^{140}Ba$ | C | | 13.8±2.7 |
| $^{131}La$ | C | 4.0±0.4 | |
| $^{132}La$ | C | 9.1±0.5 | 19.4±1.2 |



Table 2 (continued)

| 1 | 2 | 3 | 4 |
|---|---|---|---|
| $^{132}Ce$ | C | | 6.0±1.9 |
| $^{133}Ce$ | C | 8.4±1.2 | 19.9±2.8 |
| $^{135}Ce$ | C | 5.8±0.5 | 12.3±1.6 |
| $^{138}Pr^{m}$ | C | | 3.1±1.8 |
| $^{145}Eu$ | C | 13.5±1.9 | 19.3±2.7 |
| $^{146}Eu$ | C | 10.5±1.2 | 21.0±2.8 |
| $^{147}Eu$ | C | 14.1±1.6 | 29.7±3.8 |
| $^{148}Eu$ | I | | 2.3±0.4 |
| $^{150}Eu$ | C | 4.9±1.0 | 7.5±2.0 |
| $^{147}Gd$ | C | 10.8±1.2 | 25.7±3.1 |
| $^{149}Gd$ | C | 14.2±1.8 | 29.9±4.0 |
| $^{151}Tb$ | C | 8.0±3.5 | 17.3±6.9 |
| $^{153}Dy$ | C | 5.8±1.9 | 15.0±4.8 |
| $^{160}Er$ | C | 8.1±1.2 | 14.9±2.6 |
| $^{161}Er$ | C | 11.9±3.1 | 24.8±9.0 |
| $^{166}Yb$ | C | 26.1±4.9 | 47.0±9.8 |
| $^{169}Yb$ | C | 4.7±0.6 | 10.3±1.5 |
| $^{171}Lu$ | C | 17.0±1.5 | 31.7±3.3 |
| $^{170}Hf$ | C | 14.4±3.6 | 43.2±9.4 |
| $^{173}Hf$ | C | 15.3±2.0 | 36.1±4.9 |
| $^{175}Hf$ | C | 18.3±1.9 | 43.6±4.9 |

Table 2 (continued)

| 1 | 2 | 3 | 4 |
|---|---|---|---|
| $^{174}$Ta | C | 8.6±1.1 | 23.8±3.2 |
| $^{175}$Ta | C | 19.3±1.8 | 41.2±5.1 |
| $^{178}$Ta$^{m}$ | I | | 12.0±3.5 |
| $^{182}$Ta | C | | 3.9±0.7 |
| $^{182}$Re | I | | 24.1±8.2 |
| $^{184}$Ir | C | | 8.4±4.1 |
| $^{192}$Au | C | | 19.9±4.5 |

### 3.3 Charge and Mass Distributions

The nuclidic formation cross sections $\sigma(A,Z)$ were parametrized as a function of the product mass A and atomic number Z as

$$\sigma(A,Z) = \sigma(A)[2\pi C_z^2(A)]^{-1/2} \exp[-\frac{(Z - Z_p(A))^2}{2C_z^2(A)}], \quad (1)$$

where $\sigma(A)$ are isobaric yields, $C_z(A)$ is the charge dispersion width parameter for the mass number A, and $Z_p(A)$ is the most probable atomic number for that A. Over small mass ranges, the width parameter is independent of A, and the centre $Z_p(A)$ of charge distributions can be represented by a linear function of

$$Z_p(A) = a + bA. \quad (2)$$

Using these assumptions as well as a further assumption that $\sigma(A)$ varies smoothly and slowly as a function of mass number, the measured cumulative cross sections were iteratively corrected for precursor $\beta$-decay [15].

In order to obtain the charge dispersion parameters, the measured nuclidic cross sections $\sigma(A,Z)$ placed in eight groups



Table 3. Charge-dispersion parameters

| Mass range | Protons $C_z$ | a | b | Mass range | $^{12}$C-ions $C_z$ | a | b |
|---|---|---|---|---|---|---|---|
| 24-65 | 0.68 | 0.60 | 0.44 | 24-65 | 0.62 | -1.12 | 0.48 |
| 71-81 | 1.06 | 0.31 | 0.45 | 72-81 | 1.12 | 1.24 | 0.43 |
| 84-90 | 0.62 | -0.55 | 0.48 | 84-90 | 0.64 | 1.10 | 0.44 |
| 93-105 | 0.90 | -2.29 | 0.46 | 93-105 | 0.95 | 0.24 | 0.44 |
| 121-135 | 1.25 | 3.42 | 0.40 | 125-135 | 0.60 | 1.50 | 0.42 |
| 145-153 | 1.10 | 3.27 | 0.42 | 145-153 | 1.20 | 1.80 | 0.42 |
| 155-170 | 0.60 | 0.78 | 0.41 | 155-170 | 0.65 | -5.82 | 0.46 |
| 171-175 | 0.90 | -2.84 | 0.43 | 171-192 | 1.20 | -7.62 | 0.48 |

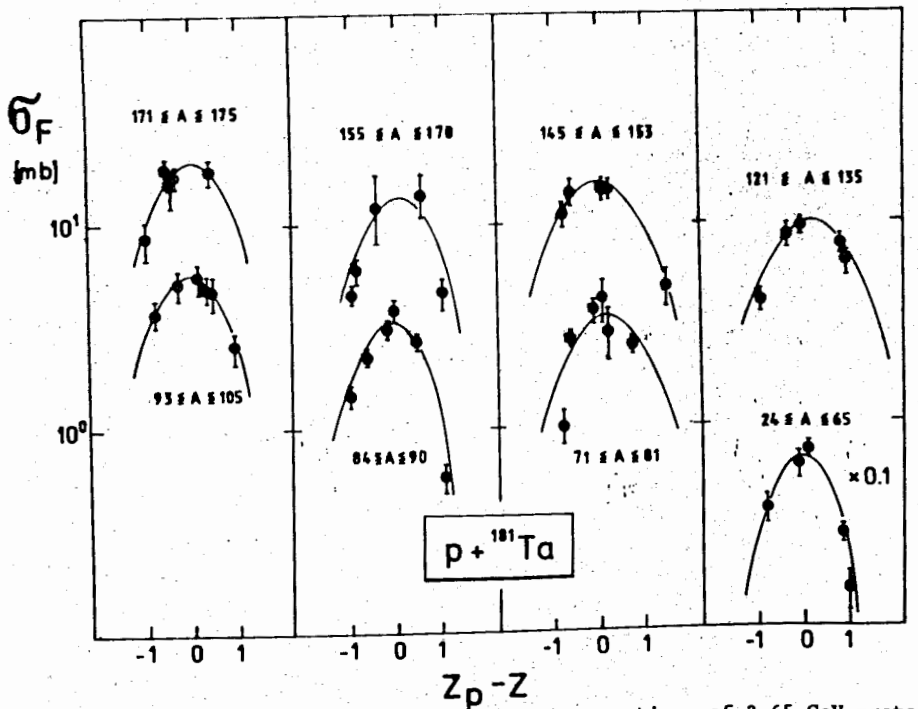


Fig. 2. The charge dispersion curves from the reactions of 3.65 GeV protons with $^{181}$Ta.

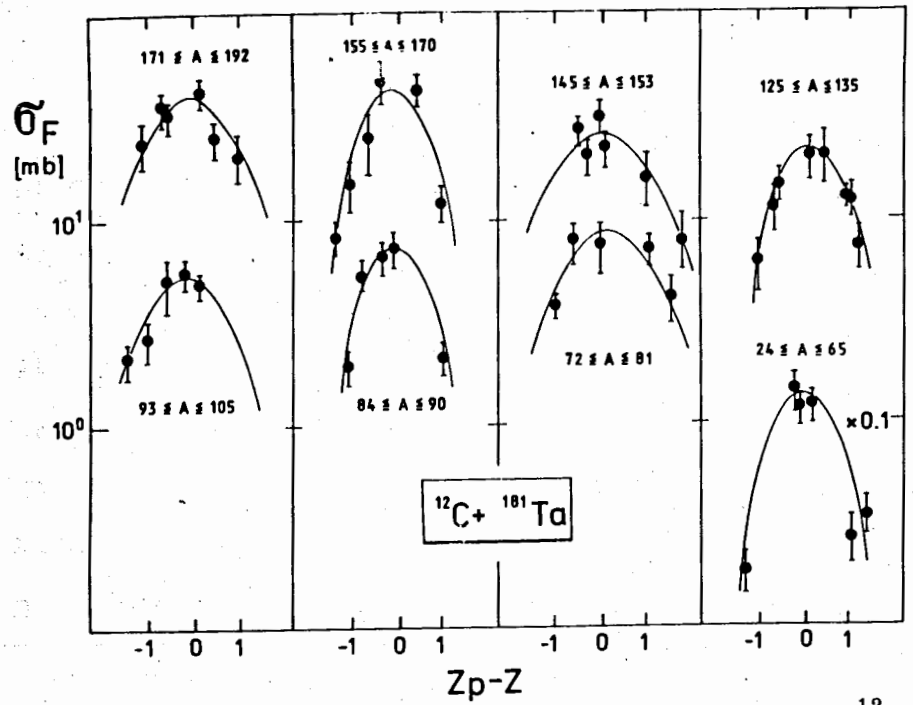


Fig. 3. The charge dispersion curves from the reactions of 3.65 AGeV $^{12}C$-ions with $^{181}Ta$.

to mass numbers were fitted to an independent Gaussian-shaped yield (eq. (1)) with the non-least-square robust minimization code ROLSM /16/. It should be noted that no isomeric states were included in the fitting procedure. Nucliding groupings along with the width parameters $C_z$ and the coefficients a and b of the $Z_p(A)$ functions (eq. (2)) for both investigations are listed in table 3. The charge distributions for target residues from the $p + ^{181}Ta$ and $^{12}C + ^{181}Ta$ reactions at 3.65 AGeV are displayed in figs. 2 and 3, respectively, where, as usual, the calculated fractional isobaric yields $\sigma_F$ are plotted versus $Z_p - Z$. As can be seen, the charge distributions of target residues from both reactions are very similar, the differences being in the magnitude of yields.

The mass isobaric yields $\sigma_A$ have been also obtained on the assumption of Gaussian charge dispersions and the set of the fitting parameters listed in table 3. The $p + ^{181}Ta$ and $^{12}C + ^{181}Ta$ mass yield distributions are displayed in fig. 4, were the $\sigma_A$ values are plotted versus the product mass number A. Both distributions are displaced vertically by a factor of 10



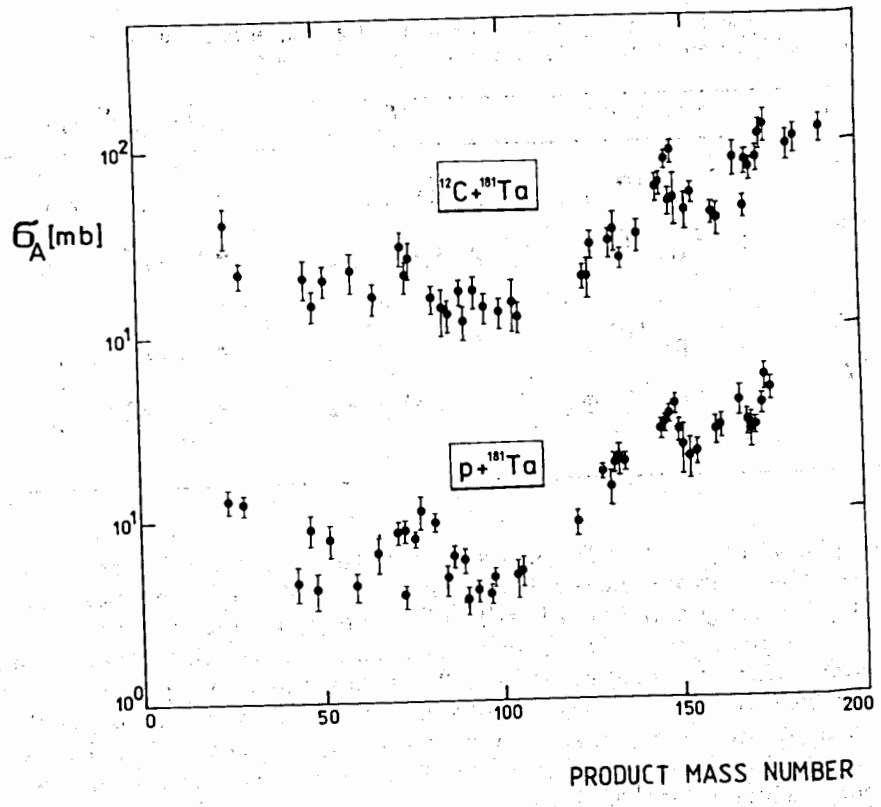


Fig. 4. The mass yield distributions of target residues from the reactions $^{12}C + ^{181}Ta$ and $p + ^{181}Ta$ at 3.65 AGeV, respectively.

for display purposes. The error bars incorporate only measurement statistics and do not take into account the errors due to uncertainties in the beam flux or those induced by the analysis of the charge distributions. Due to the charge dispersion fitting process, the value of systematic uncertainties was estimated to be approximately 20%.

### 3.4. Recoil Properties of Intermediate Fragments

The Mylar foils No.4 and No.8 in both target stacks were used as catchers of intermediate fragments ($^{24}Na$, $^{28}Mg$) emitted in the backward and forward direction, respectively. The appropriate forward (F) and backward (B) catcher foils were gamma-ray counted on the same Ge(Li) spectrometer as discussed in Sect. 2. The activities of $^{24}Na$ and $^{28}Mg$ were determined in a given catcher from the counting rates of the most in-

Table 4. Recoil properties of $^{24}$Na and $^{28}$Mg fragments produced in the p + $^{181}$Ta and $^{12}$C + $^{181}$Ta reactions at 3.65 AGeV

| Fragment | Reaction | F/B | 2W(F+B) (mg/cm$^2$) |
|---|---|---|---|
| $^{24}$Na | p + $^{181}$Ta | 2.01±0.11 | 10.56±1.45 |
| | $^{12}$C + $^{181}$Ta | 2.32±0.14 | 12.88±1.67 |
| $^{28}$Mg | p + $^{181}$Ta | 1.86±0.12 | 12.48±1.50 |
| | $^{12}$C + $^{181}$Ta | 2.20±0.14 | 14.23±1.73 |

tense gamma-rays [14]. It makes possible to determine the ratios of the forward-to-backward emission F/B and the mean ranges in the target material 2W(F+B). Here, F and B are the fractional numbers of fragments recoiling into the forward and backward catcher, respectively, W is the total target thickness in mg/cm$^2$. The results obtained for $^{12}$C-ion and proton projectiles are summarized in table 4. It is seen that F/B as well as 2W(F+B) values for both fragments are larger in reactions induced by $^{12}$C-ions.

## 4. TEST OF FUNDAMENTAL HYPOTHESES

The discussion of results can be presented in terms of the basic concepts of high-energy nuclear physics, such as factorization and limiting fragmentation.

Let us consider a single particle inclusive reaction

$$P + T \longrightarrow F + X, \qquad (3)$$

in which the projectile P interacts with the target T to produce fragment F, and X represents anything else. Following the hypothesis of factorization [5], the cross section for product of the target fragmentation F can be factorized to

$$\sigma^F_{T,P} = \sigma^F_T \gamma_P, \qquad (4)$$

where $\gamma_P$ is dependent only on the projectile. Thus, the factorization implies that ratios



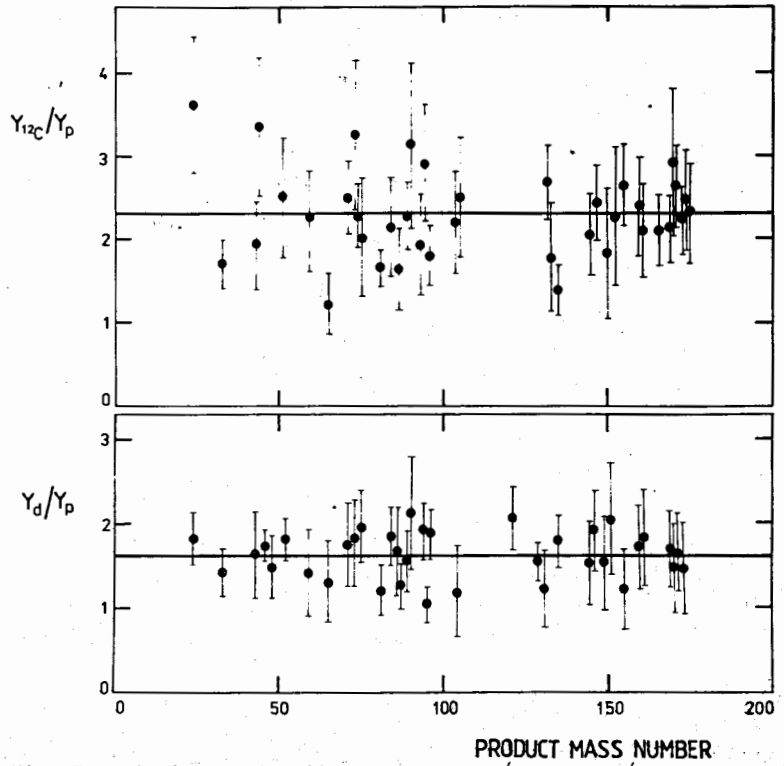


Fig. 5. Relative projectile factors $\gamma_{12C}/\gamma_p$ and $\gamma_d/\gamma_p$ of target residues from the reactions of 3.65 AGeV $^{12}$C-ions, deuterons [11] and protons with $^{181}$Ta. The solid horizontal lines indicate the appropriate average values.

$$\frac{\sigma^F(^{12}C + ^{181}Ta)}{\sigma^F(p + ^{181}Ta)} = \frac{\gamma_{12C}}{\gamma_p}, \qquad (5)$$

should have a constant values for any target residue. In the equation (5) the ratio $\gamma_{12C}/\gamma_p$ represents a relative projectile factor. This observable for tantalum fragmentation by 3.65 AGeV $^{12}$C-ions and 3-65 GeV protons is displayed in fig.5. The average value of the relative projectile factor $\langle\gamma_{12C}/\gamma_p\rangle = 2.32 \pm 0.56$ was obtained for 38 values of isobaric cross sections of target residues in the mass region from A = 24 to A = 175. It corresponds to the ratio of the total cross sections of monitoring reactions $^{27}$Al($^{12}$C,X)$^{24}$Na and $^{27}$Al(p,X)$^{24}$Na at 3-65 AGeV which is 2.18 ± 0.39. The relative projectile factors $\gamma_d/\gamma_p$ for 3-65 AGeV deuterons [11] and 3-65 GeV protons

Table 5. Comparison of cross sections, radii and impact parameters of nuclear reactions with $^{181}$Ta induced by 3.65 AGeV protons, deuterons /11/ and $^{12}$C-ions

| Reaction | $\sigma^{TR}$ (b) | $\sigma_R$ (b) | $R_P$ (fm) | $R_T$ (fm) | b (fm) |
|---|---|---|---|---|---|
| p+$^{181}$Ta | 1.52±0.26 | 2.22 | 1.37 | 7.75 | 6.96 |
| d+$^{181}$Ta | 1.67±0.31 | 2.42 | 1.73 | 7.75 | 7.29 |
| $^{12}$C+$^{181}$Ta | 2.36±0.48 | 3.26 | 3.14 | 7.75 | 8.67 |

are also shown in fig. 5. The average value $\langle \gamma_d/\gamma_p \rangle = 1.62 \pm 0.39$ was found to be also consisted with the ratio of total cross sections of appropriate monitoring reactions which is $1.70 \pm 0.32$ /17/.

The production cross section of target residues, $\sigma^{TR}$, can be obtained by an appropriate summing of the isobaric yields. Our integration was performed over the interval from A = 40 to the target mass number. A lower limit of 40 mass units was chosen for the same reasons as given in /18/. The results of this integration along with those for the d + $^{181}$Ta /11/ investigation are summarized in table 5. Here, the total reaction cross sections $\sigma_R$ calculated as

$$\sigma_R = \pi r_o^2 (A_P^{1/3} + A_T^{1/3} - b_{PT})^2, \qquad (6)$$

with parameters $r_o = 1.37$ fm and $b_{PT} = 0.51$ /19/ are also included. The scaling of the cross sections $\sigma^{TR}$ is evident. It is also seen that cross sections of target residues represent about 70% of $\sigma_R$; from the fraction of the total reaction cross section the impact parameter b can be estimated. As is seen from table 5, the calculated impact parameter values $b < R_P + R_T$, where the appropriate radii are $R_P = r_o A_P^{1/3}$ and $R_T = r_o A_T^{1/3}$, respectively. This indicates that residues from the tantalum fragmentation by 3.65 AGeV projectiles are produced in collisions where the centre of the projectile lies inside the radius of the target nucleus.

Another evidence for factorization could follow from the comparison of F/B and 2W(F + B) recoil properties for both



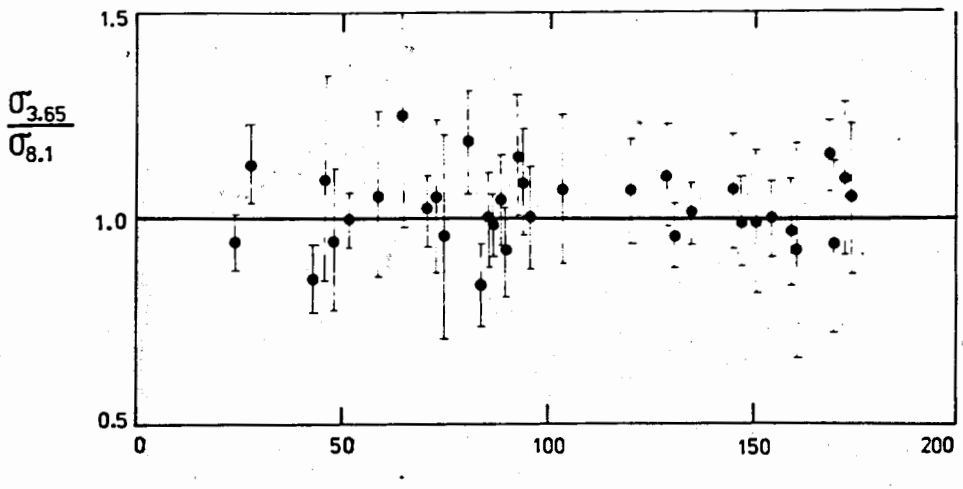


Fig. 6. Ratios of cross sections of target residued from p + $^{181}$Ta reactions measured in this work with 3.65 GeV protons to those of ref. /11/ for 8.1 GeV.

projectiles. If the factorization hypothesis is valid, the appropriate ratios should oscillate about unity:

$$\frac{[F/B]_{^{12}C}}{[F/B]_p} = \frac{[2W(F+B)]_{^{12}C}}{[2W(F+B)]_p} = 1. \qquad (7)$$

Nevertheless, the ratios $[F/B]_{^{12}C}/[F/B]_p$ for $^{24}$Na and $^{28}$Mg fragments $1.15 \pm 0.14$ and $1.18 \pm 0.16$, respectively, as well the ratios of mean ranges $[2W(F+B)]_{^{12}C}/[2W(F+B)]_p$ $1.22 \pm 0.34$ and $1.14 \pm 0.29$, respectively, are larger than expected.

The concept of limiting fragmentation /6/ implies that for sufficiently high projectile energies the cross section for production of a residue is independent of energy. In order to test this hypothesis, we compared our p + $^{181}$Ta results with previous proton data /10,11/ at 5.7 GeV and 8.1 GeV, respectively. The ratios $\sigma_{3.65}/\sigma_{5.7}$ and $\sigma_{3.65}/\sigma_{8.1}$ (see fig. 6) of the measured 10 and 34 nuclidic cross sections, respectively, fluctuate about unit. The average values of the ratios are

$$\langle \sigma_{3.65}/\sigma_{5.7} \rangle = 1.05 \pm 0.15$$

$$\langle \sigma_{3.65}/\sigma_{8.1} \rangle = 1.05 \pm 0.29,$$

respectively. The target residue mass distributions obtained for the reaction of relativistic protons with tantalum target nuclei are compared with those for intermediate protons [7-9] in fig. 7. The shapes of p + $^{181}$Ta mass yield distributions at 3.65 GeV, 5.7 GeV and 8.1 GeV are very similar, but different from those resulting from the p + $^{181}$Ta reactions at 0.34 GeV [7], 0.45 GeV [8] and 0.66 GeV [9] proton energies. The limiting fragmentation, as has been attempted, is not valid for intermediate proton energies. The similarity of the mass distributions of target residues as well as ratios of nuclidic cross sections at 3.65 GeV, 5.7 GeV and 8.1 GeV manifests the validity of limiting fragmentation at these energies.

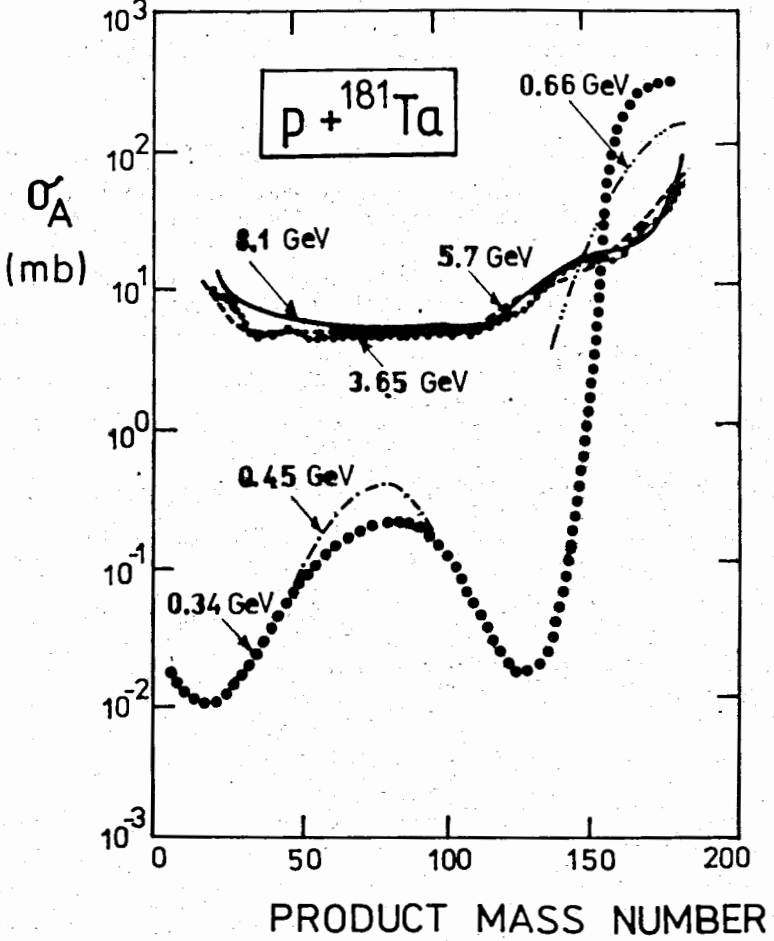


Fig. 7. The comparison of the target residue mass distributions for the interactions of tantalum with intermediate and high-energy protons.



## 5. COMPAROSON WITH MODEL CALCULATIONS

The mass-yield distributions of target residues from the p + $^{181}$Ta and $^{12}$C + $^{181}$Ta reactions at 3.65 AGeV were compared with the abrasion-ablation (AA) and intranuclear cascade (INC) model calculations. These two models represent two different views of relativistic nuclear collisions: while the intranuclear cascade model pictures the interaction as uncorrelated collisions between individual nuclaons from two nuclei, the abrasion-ablation model assumes that the interaction consists of inelastic collisions of "streaks" of nuclear matter with an overlap region. Both model representations are based on the same assumption that the nuclear reaction is a two-stage process. In the first fast stage of the interaction an excited primary projectile and target remnants are created, in the second stage a slow statistical deexcitation of the remnants by particle emission is followed.

The collision in the INC model is governed by the properties of the nucleon-nucleon interaction: each nucleon from the projectile and target interacts as a single entity. A detailed review of different approaches and many generalizations of this model can be found in ref. [20]. The version of the INC model and appropriate computer codes that we have used are those of Hanssgen et al. [21-28] . Because the model approaches have been described in detail in refs. [21-24] , only the main assumptions are presented here. The INC-codes HADRIN [26], NUCRIN [27] and JADJAD [28] provide a Monte-Carlo (MC) simulation of the inelastic hadron-nucleon, hadron-nucleus and nucleus-nucleus interactions, respectively, of the type

$$A_1 + A_2 \rightarrow \sum_i h_i + F; \qquad (8)$$

the statistical decay is performed by the MC-code DECAY [25].

The colliding nuclei, considered in their rest systems with uniform nucleon density distributions, are divided into central and peripheral interaction regions. While in the central region the fractions of both colliding nuclei interact together in row-on-row picture [29], the remaining fragments outside the central region interact only with one single nucleon. The impact parameter and azimuthal angle are determined by the MC sampling, the average scattering angle is determined from the nucleon-nucleon interaction. The size of the central region of the interaction is assumed to be proportional to the volume of the corresponding developed cascade cone which depends on the laboratory momentum of the projectile and the

number of nucleons of the target nucleus. For uniform nucleon distributions inside the nucleus the number of nucleons in the central region is proportional to the volume of this cone and can be calculated by the corresponding geometrical conditions. The corresponding nucleon Fermi momenta are MC sampled from the phase-space momentum distribution. The simulation stops, if no further nucleon is available inside one of the colliding nuclei or if energy and charge conservation do not allow any further particle emission. The appropriate formulae used for the calculation of excitation and cascade energies can be found in [21]. The Pauli pronciple is applied only for nucleons and interactions between cascade hadrons are neglected.

The application of the macroscopic AA model in target fragmentation calculations must be connected with the simple "clean-cut" geometry [30-32]. We have used the "firestreak" geometry [33] to calculate the abrasion stage of the interaction. From this part of the calculation we obtained the excitation energies and cross section for the formation of the primary residues. In the ablation stage of the interaction the primary residues were deexcited through the statistical evaporation in order to construct the final product residue mass distribution from the primary distribution and the excitation energy of each primary.

Two basic assumptions were included: both nuclei were assumed to have sharp spherical surfaces and the interaction proceeded via collinear streaks of nuclear matter from the projectile and target. The colliding nuclei with radii equal to $1.37A^{1/3}$ and streaks of $0.15 \times 0.15$ fm$^2$ were taken into account in our calculations. Each of the streaks consisted of the sum $N_P + N_T$ of participant nucleons from the projectile, $N_P$, and target, $N_T$, respectively. This sum was calculated from geometrical considerations alone as a function of the impact parameter b. From the inverse function of b the cross section for a primary residue of a given mass has been determined. Each primary residue was assumed to have an excitation energy given by multiplying the surface energy coefficient 0.95 MeV/fm$^2$ [34] by the excess surface area of the residue. The deexcitation of the primary residues has been calculated using a modified version of the well-known evaporation code ALICE [35]. We used the level density

$$\rho(E^*) = C(E^*)^{-2} \exp[2\sqrt{aE^*}], \qquad (9)$$

where C is a constant proportional to mass number and $a = A/8$ MeV$^{-1}$. The cross sections of the final products were



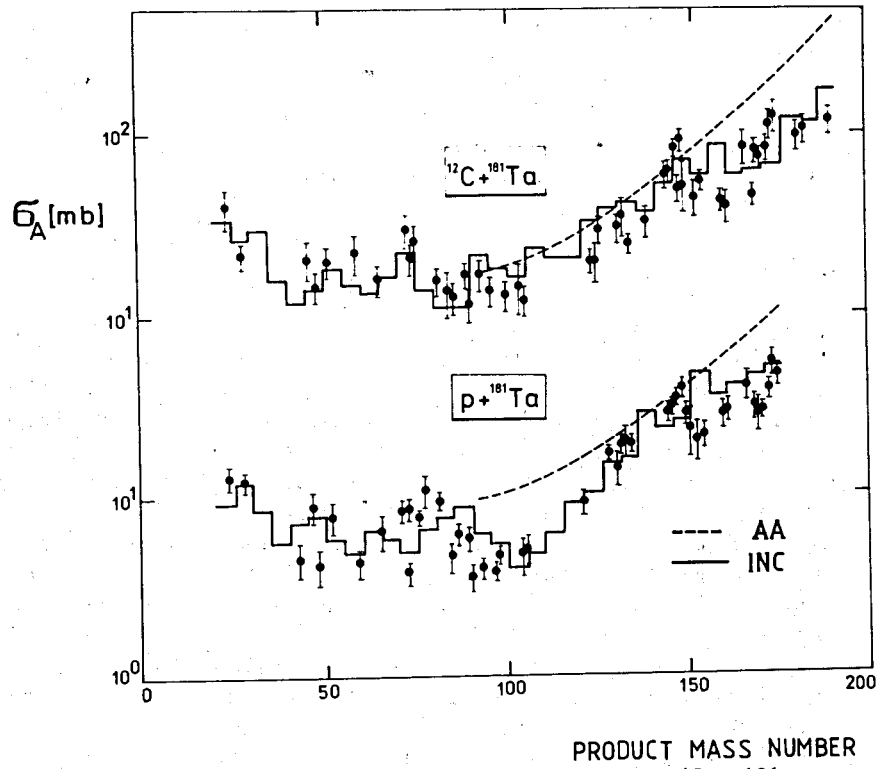


Fig. 8. The comparison of the mass distributions from $^{12}C + ^{181}Ta$ and $p + ^{181}Ta$ reactions at 3.65 AGeV with INC (solid histograms) and AA (dashed curves) calculations.

obtained by the appropriate summing over the impact parameter of the initial collision, each impact parameter being weighted by its geometrical probability.

The mass distributions calculated for the nuclear reactions $^{12}C + ^{181}Ta$ and $p + ^{181}Ta$ at 3.65 AGeV using the INC and AA models are compared to experimental isobaric cross sections in fig. 8. The INC calculated results have been bined in $\Delta A = 4$ intervals, the results of the AA calculation in the firestreak geometry are shown by the dashed lines. We have arbitrarily cut off the AA calculations at $A \approx A_{target}/2$ because the emission of products with lower mass lies outside the scope of the AA model [34,36]. A good general agreement with the experimental mass-yield distributions was obtained. Particularly, the INC model reproduces both experimental mass-yield distributions reasonably well. On the other hand, the AA firestreak model calculations were found to overestimate the appropriate mass-yield distributions in the vicinity of the

target mass numbers. The discrepancies between calculated and experimental values in the target mass regions are caused by the low values of the excitation energies of the abraded nucleus. Nevertheless, the shift to higher values of excitation energies predicted by this model is unrealistic and it destroys the shape of the AA model curve, as well.

## 6. CONCLUSIONS

The determination of nuclidic cross sections of many target residues from the interaction of tantalum with 3.65 AGeV $^{12}$C-ions and protons as well as attentive parametrization of these data enabled us to perform a detailed comparison of the interaction of these two projectiles with a heavy target nucleus. The charge dispersions were found to be closely comparable and the mass-yield distributions obey factorization down to A ~ 30. The intermediate mass fragments $^{24}$Na and $^{28}$Mg have enhanced forward-to-backward ratios and mean ranges in $^{12}$C-ion induced reactions. The evidence of limiting fragmentation comes from the similarity of the p + $^{181}$Ta mass distributions at 3.65 GeV, 5.7 GeV and 8.1 GeV proton energies. The integration of the cross sections for target residues with A $\geq$ 40 makes a contribution of 70% to the total reaction cross section. The calculation of the impact parameters based on this fraction of the "Hard sphere" reaction cross section indicates that target residues from the reactions of 3.65 AGeV $^{12}$C-ion and proton projectiles with $^{181}$Ta nuclei are created mainly in central collisions.

The results have been compared with two different reaction models. The agreement of the mass yield distributions with intranuclear cascade calculations indicates that both interactions can be understood as uncorrelated collisions between individual nucleons from the interacting nuclei.On the other hand, the mass yield distributions predicted by the macroscopic abrasion-ablation model in a firestreak geometry were found to overestimate experimental isobaric yields, particularly in the vicinity of the target mass numbers. These discrepancies could not be explained by the increasing of the appropriate excitation energies. The introduction of the "collective tube" interaction may be an improvement in this respect.

The cooperation of Prof. K.D.Tolstov, Dr. Yu.A.Panebratsev, A.N.Khrenov, V.G.Perevozchikov and the staff of the Dubna synchrophasotron is gratefully acknowledged. Without their assistance the present work would not have been possible. Thanks are due to Drs. K.Hanssgen and R.R.Mekhtijev for performing the model calculations, and V.B.Zlokazov for the application of his ROLSM code for parametrization of nuclidic cross sections. We are also indebted to Prof. M.Suk for his interest in this work and a critical reading of the manuscript.



## REFERENCES

1. S.Fredriksson et al.- Phys. Rev., 1987, 144, p.187 and references cited here.
2. Bowman J.D., Swiatecki W.J., Tsang C.F. - Report LBL-2908, 1973, Berkeley.
3. Bertini H.W., Guthrie M.P. - Nucl. Phys., 1971, A169, p.670.
4. Yariv Y., Fraenkel Z. - Phys. Rev., 1979, C20, p.2227.
5. Feynman R.P. - Phys. Rev. Lett., 1969, 23, p.1415.
6. Benecke J. et al. - Phys. Rev., 1969, 188, p.2159.
7. Nervik W.E., Seaborg G.T. - Phys. Rev., 1955, 97, p.1092.
8. Kruger P., Sugarmann N. - Phys. Rev., 1955, 99, p.1459.
9. Labrukhin A.K., Pozdnyakov A.A. - Sov. J. of Atomic Energy, 1961, 7, p.862.
10. Grover J.B. - Phys. Rev., 1962, 126. p.1540.
11. Kozma P., Kliman J., Leonard M. - Czech. J. Phys. B, 1988, 38, p.973.
12. Damdinsuren C. et al. - JINR, P1-87-932, Dubna, 1987.
13. Koskelo M.J., Aarnio P.A., Routti J.T. - NIM, 1981, 190, p. 89.
14. Reus U., Westmeier W. - Atomic and Nucl. Data Tables, 1983, 29,p. 1.
15. Damdinsuren C. et al. - JINR, P1-88-135, Dubna, 1988; and to be published.
16. Zlokhazov V.B. - JINR, P10-86-618, Dubna, 1986.
17. Kozma P., Kliman J. - Czech. J. Phys., 1988, B38, p.1317; and to be published.
18. Morrisey D.J. et al. - Phys. Rev., 1980, C21, p.1783.
19. Heckmann H.H. et al. - Phys. Rev., 1978, C17, p.1735.
20. Barashenkov V.S., Toneev V.D. - Interactions of High Energy Particles and Atomic Nuclei with Nuclei, Moscow: Atomizdat, 1972.
21. Hanssgen K., Ranft J. - Nucl. Sci. Eng., 1984, 88, p.537.
22. Hanssgen K., Mohring H.-J., Ranft J. - Nucl. Sci. Eng., 1984, 88, p.551.
23. Grichin V.G., Hanssgen K., Kladnitskaya T.N. - JINR, E1-85-73, Dubna, 1985.
24. Hanssgen K. - Nucl. Sci. Eng., 1987, 95, p.135.

25. Hanssgen K., Ritter S. - Comp. Phys. Com., 1984, 31, p.411.
26. Hanssgen K., Ranft J. - Comp. Phys. Com., 1986, 39, p.37.
27. Hanssgen K., Ranft J. - Comp. Phys. Com., 1986, 39, p.53.
28. Hanssgen K., Ranft J. - Comp. Phys. Com.; to be published.
29. Hufner J., Knoll J. - Nucl. Phys., 1977, A290, p.460.
30. Westfall G.D. et al. - Phys. Rev. Lett., 1976, 37, p.1202.
31. Gosset J. et al. - Phys. Rev., 1977, C16, p.629.
32. Gosset J., Kapusta J.I., Westgall G.D. - Phys. Rev., 1978, C18, p.844.
33. Myers W.D. - Nucl. Phys., 1978, A269, p.177.
34. Morrissey J.D. et al. - Phys. Rev., 1978, C18, p.1267.
35. Blann M. - USAEC Report No.C00-3494-29 (unpablished).
36. L.F.Oliveira L.F., Donangelo R., Rasmussen J.O. - Phys. Rev., 1979, p.826.

Received by Publishing Department
on April 12, 1989.



Козма П. и др. E1-89-252

Реакции тантала с ядрами $^{12}C$ и протонами с энергиями 3.65 АГэВ и 3.65 ГэВ

Сечения образования ядер-остатков при взаимодействии ядер тантала с ядрами $^{12}C$ и протонами с энергией 3,65 АГэВ определены по измерению гамма лучей с использованием Ge(Li) спектрометра. На основе этих данных определены зарядовые и массовые распределения образовавшихся ядер-остатков. Анализ экспериментальных результатов проводится в рамках основных концепций физики фрагментации при высоких энергиях. Данные также сравниваются с расчетами по теоретической модели обдирки и внутриядерного каскада.

Работа выполнена в Лаборатории высоких энергий ОИЯИ.

Препринт Объединенного института ядерных исследований. Дубна 1989

P.Kozma et al. E1-89-252

Nuclear Reactions of Tantalum with 3.65 AGeV $^{12}C$-Ions and 3.65 GeV Protons

The cross sections of a number of target residues formed in the reactions of 3.65 AGeV $^{12}C$-ions and 3.65 GeV protons with tantalum have been measured. The measurements have been done by direct counting of irradiated targets with a Ge(Li) gamma-ray spectrometer. Charge dispersions and mass-yield distributions were deduced from these data. The results are discussed in terms of the basic concepts of high-energy nuclear physics. They are also compared with intranuclear cascade and abrassion-ablation model calculations.

The investigation has been performed at the Laboratory of High Energies, JINR.

Preprint of the Joint Institute for Nuclear Research. Dubna 1989